Chemostratigraphy and Mineralogy of Shales Penetrated by Akukwa and Amansiodo Wells in the Anambra Basin, SE Nigeria

[1]Haruna, K. A* and [2]Ojo, O. J
[1]Al-Hikmah University, Ilorin, Nigeria.
[2]Federal University Oye-Ekiti, Ekiti State, Nigeria

ABSTRACT

Geochemical and mineralogical analyses of shales penetrated by Akukwa and Amansiodo wells of Anambra Basin in the context of paleoenvironments and chemostratigraphy. Sixty well samples were subjected to XRF, ICMPs and XrD analyses. Major Oxides and Rare Earth Elements were used to construct chemostratigraphic profiles for the investigated wells in the study area. Four chemo zones were identified for each of the wells. AK1 is characterized by high CaO, P_2O_5 and low NA_2O, K_2O and SiO_2 indicating marine transgression while Zone AK_2 is characterized by high SiO_2, K_2O, Na_2O, Al_2O_3 and low CaO, MgO and P_2O_5 indicating a regression of the marine environment. Zone AM1 is characterized by high MgO, CaO, P_2O_5 and low SiO_2, K_2O indicating marine transgression while AM_2 is low in MgO, CaO, P_2O_5 and high SiO_2 indicating regression. The Sr/Ba ratios in Akukwa ranges from 0.21-0.63 indicating a fresh-brackish water environment while Sr/Ba ratios in the Amansiodo wells ranges from 0.22-1.29, indicating saline conditions. The value of Boron content as well as the Boron/Gallium (B/Ga) ratios in Akukwa samples are 33.1-57.9 µg/g and 1.30-2.89 respectively while Amansiodo well are 19.2-86.7 µg/g and 1.09-35.22 indicating brackish water environment. Values of V/(V+Ni) for Akukwa well samples range from 0.39-0.45 with average of 0.42 while in Amansiodo, it ranges from 0.40-0.88 with average of 0.45 suggesting oxic condition. In Akukwa well, the mean values of Ni/Co: (2.49), V/Cr (1.04) Cu/Zn (0.37) Cu+Mo/Zn: (0.39) are slightly higher than mean values in Amansiodo (Ni/Co: 2.31, V/Cr: 0.97, Cu/Zn: 0.34, (Cu+Mo)/Zn: 0.37), pointing to an oxic conditions. The presence of kaolinite in all the analysed intervals and few smectite is interpreted to be suggestive of exhaustive leaching under acidic tropical conditions while the presence of halite and gypsum in some intervals suggest sedimentation in an isolated density-stratified, sediment starved and stagnant conditions.

Keywords: Chemostratigraphy, Mineralogy, Amansiodo, Akukwa, Paleoenvironments

INTRODUCTION

A stratigraphic record is the result of an exogenous mechanism (one from outside) consisting of geological setting, sea level changes, changes in geochemical reactions between seawater and rock, processes of climate and sediment formation (Srinivasan, 1989), so differences in bulk chemistry are exposed by the resulting sedimentary record. Furthermore, because these modifications produce various mineral combinations, the sediment's distinctive main and trace elemental compositions are also observable and can be used to compare and classify these rocks; this, in turn, forms the basis for applying chemostratigraphy in subdividing strata (Das, 1997). With the ability to analyse these distinctions, the concept of chemostratigraphy holds well the distinction between chemical composition and its causative factor (local, regional or global), enabling chemozone identification and analysis on an adequate scale (Ramkumar & Sathish, 2006).

Inorganic geochemical studies of sedimentary sequences, also known as chemostratigraphy, can be used as a reference method for researching changes in the geochemistry of sediments. This is achieved by analysing samples of conventional core samples, ditch cutting, sidewall core and outcrop samples that allow inter-well correlations to be made at the regional to reservoir scale. It includes the Application of geochemistry of the major- and trace elements to classify and subdivide sequences into distinct geochemical units and strata differentiation in sedimentary basins. It is a robust technique that uses changes in abundance of the major, trace and rare earth elements to classify and correlate sedimentary rock sequences. Chemostratigraphy stratigraphic technique is

The authors wish to thank NNPC Limited, NNPC Upstream Investment Management Services (NUIMS), Al-Hikmah University, Ilorin, Nigeria. Federal University Oye-Ekiti, Ekiti State, Nigeria and NAPE for providing the platform to present the paper during the Annual Conference.

based on identifying shifts in the Concentration of elements over time and using them to model shifts in geological events such as provenance (Ratcliffe *et. al.,* 2010; Pearce *et. al.,* 2005) and paleoclimate (Wright *et. al.,* 2010; Ratcliffe *et. al.,* 2007).

The correlation of Chemostratigraphic data is especially applicable to sequences with very little biostratigraphic control or sequences that are very thick, deposited rapidly and cannot be further subdivided by biostratigraphic data. In addition, uncertainty and more conventional correlation approaches such as biostratigraphy, lithostratigraphy, and geophysical logging are also overcome.

GEOLOGY AND LOCATION OF THE STUDY AREA

The study area in the southern part of the regionally wide northeast-southwest of Benue Trough is the Anambra Basin (Figure 1), a Cretaceous Basin. It is a synclinal structure consisting of upper Cretaceous to Recent sediments over 5,000 ft thick, and it represents the third phase of marine sedimentation in the Benue Trough after the Santonian Tectonic event (Ladipo, 1988; Akande & Erdtman, 1998; Ojo *et. al.,* 2009, 2010). Consequently, the basin was believed to have evolved into the late Jurassic to the Cretaceous basement fragmentations with subsidence, rifting, block faulting and drifting apart from the South American and African plates and thus represent part of the West African Rift System (Genik, 1992; Fairhead & Okereke, 1987; Ojo *et. al.,* 2009). The stratigraphic sequence in the basin-reveals that the basin consists of the Enugu/Nkporo/Owelli Campanian to Maastrichtian Type. The study wells lay within the Enugu Sheet 72 of the Nigerian Geological Survey Agency (NGSA) of 1957 and were compiled by Shell-BP Petroleum Development Company of Nigeria Limited. The well Amansiodo-1 lies within 60 28.7'N and 70 16.9'E, while the well Akukwa-2 lies within 60 15.9'N and 70 9.87'E (Figure 2).

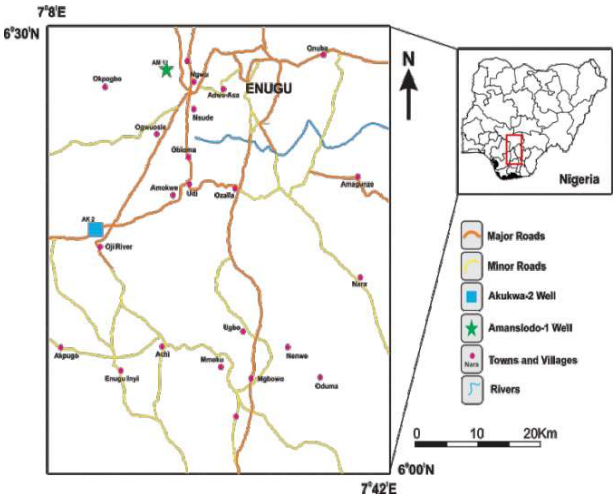

Figure 2: Location Map of the Study Area Extracted from Enugu sheet 72 of Nigerian Geological Survey Agency.

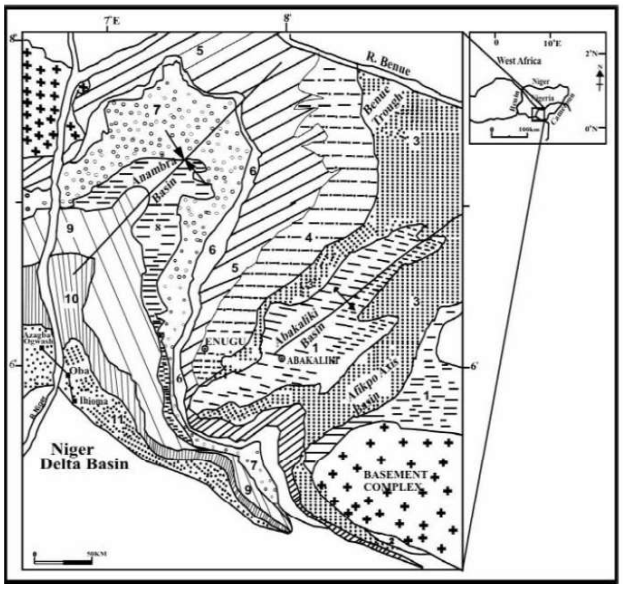

Figure 1: Generalised geological map of Anambra Basin (boxed area of inset) (Akande *et al.,* 2007) 1. Asu River Group, 2. Odukpani Fm., 3. Eze-Aku Shale, 4. Awgu Shale, 5. Enugu/Nkporo Shale, 6. Mamu Fm., 7. Ajali Sandstone, 8. Nsukka Fm., 9. Imo Shale, 10. Ameki Fm., 11. Ogwashi Asaba Fm.

METHODS

Approximately 60 shale samples were collected from the two wells for this study. Their mineralogical composition was studied at Bureau Veritas, Vancouver, Canada. The samples were tested using two methods for Major Elements (Oxides), Rare Earth Elements (RRE) and Trace elements (TE); Aqua regia ultra-trace Inductively Coupled Plasma Mass Spectroscopy (ICP-MS) and X-ray Fluorescence (XRF).

RESULTS AND DISCUSSION

Chemostratigraphic profiles provide an instrument for detecting geochemical events that are stratigraphically important. These events are usually marked in elementary curves by either maxima or minimum deflections. However, based on interpretations from the graphical analysis of the geochemical data of the sediments and the chemostratigraphic correlation, various zones have been established and will be analyzed accordingly:

CHEMOSTRATIGRAPHIC ZONES WELLAKUKWA-2

Geochemical data from the borehole resulting from the shale samples are described in Figures 3 - 5. It presents the

geochemical profiles against the depth of the absolute elementary concentrations. This approach allows the visualization of the main geochemical features of the study intervals. They are centered on elementary depletions, enrichments, and the evolution of recurrent patterns recognized from the geochemical profiles. The research profiles are divided into intervals called 'chemostratigraphic units' that are geochemically distinct. The average concentrations of elements for each unit are shown in Tables 1 - 3. The interval of study is divided into four chemostratigraphic units. The boundaries between the chemostratigraphic units broadly coincide with the limits of the lithostratigraphy. The principal geochemical characteristics of these units are shown below:

UNIT AK1

This unit is characterized by high values for SiO_2, Al_2O_3, TiO_2, Na_2O, Cr/Sc, Zr/La, TiO_2/K_2O, TiO_2/Zr, NaO/TiO_2, Zr, Cr, Cu and low values for MgO, MnO, Fe_2O_3, CaO, K_2O, P_2O_5, Zr/Cr, Sc/Zr, Zn/Sc, TiO_2/K_2O, Fe_2O_3/MgO, log (Zr/Al_2O_3), Ba, La, Ce, Sc, Sr, Y, Zn. The high values for SiO_2 and Al_2O_3 and low values for CaO and MgO can be suggested to correspond to marine regression and a high supply of continental sediments. This was observed within the plots of major elements, trace elements and their ratios.

UNIT AK2

The unit begins from about 900m and extends to 1300m within the well Akukwa-2; it has high values for CaO, MgO, P_2O_5, TiO_2, MgO, CaO, MnO, P_2O_5, Zn/Cr, Zr/La, Cr/Sc, Sc/Zr, TiO2/Zr, Log (Zr/Al_2O_3), TiO_2/K_2O, Fe_2O_3/MgO, Zr, Ba, Cr, Cu, Ce and low values for SiO_2, Al_2O_3, Fe_2O_3, Na_2O, Zn/Sc, NaO/TiO_2, La, Sc, Sr, Y and Zn. The high values for CaO, MgO, and P_2O_5 and low values for SiO_2, Al_2O_3, Fe_2O_3, and Na_2O suggest being characterized by marine transgression. The unit can also be suggested to experience maximum flooding surface (MFS) around 1200m within the well.

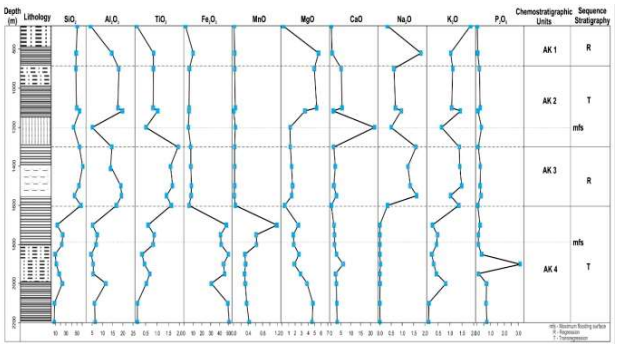

Figure 3: Major Element Geochemical Profiles for Well Akukwa-2.

UNIT AK3

The unit begins from about 1300m to 1600m within the well Akukwa-2. It has high values for SiO_2, Al_2O_3, TiO_2, Na_2O, K_2O, Zr/Cr, Cr/Sc, Zr/La, TiO_2/K_2O, Log(Zr/Al_2O_3),

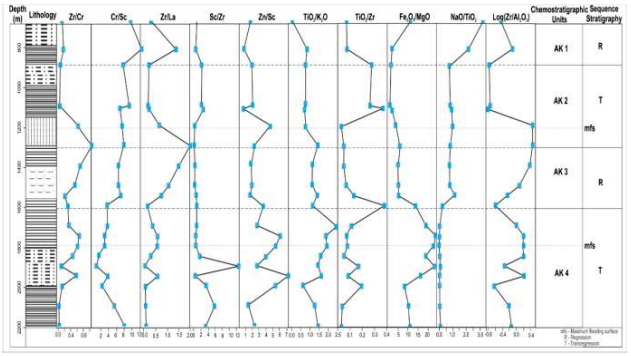

Figure 4: Ratio Geochemical Profiles for Well Akukwa-2.

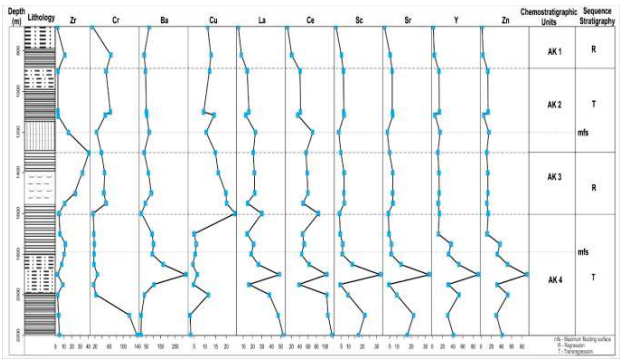

Figure 5: Trace Element Geochemical Profiles for Well Akukwa-2.

Zr, Cr, Cu, La, Ce and low values for Fe_2O_3, Mno, MgO, CaO, P_2O_5, Sc/Zr, Zn/Sc, TiO_2/Zr, Ba, Sc, Sr, Y and Zn. This zone is suggested to correspond to marine regression as a considerable reduction was observed in the values of CaO, MgO, P_2O_5, and high values for SiO_2 and Al_2O_3.

UNIT AK4

This begins from 1600m and runs down to the bottom of the well. It has high values for MnO, MgO, P_2O_5, TiO_2, Fe_2O_3, MnO, Zn/Sc, Sc/Zr, TiO_2/K_2O, Fe_2O_3/MgO, log (Zr/Al_2O_3), Ba, La, Sc, Sr, Y, Zn and low values for Al_2O_3, SiO_2, Na_2O, K_2O, Zr/Cr, Cr/Sc, Zr/La, TiO_2/Zr, Nao/TiO_2, Zr, Cr, Cu, Ce. This zone suggests being characterized by marine transgression as there is a high value for marine-derived elements as confirmed by major, trace and ratio plots.

WELL AMANSIODO-1

Table 1: Akukwa Major Element Geochemical Profiles.

UNITS	SiO_2	Al_2O_3	TiO_2	Fe_2O_3	MnO	MgO	CaO	Na_2O	K_2O	P_2O_5
AK 1	50	15	0.7	15	0.1	6	1	1.8	1.7	0.1
AK 2	53	20	1	10	0.15	6	25	1	1.3	0.5
AK 3	55	20	2	10	0.1	2	5	1.6	1.5	0.5
AK 4	10	12	0.9	50	1.2	5	6	0	1	3

The analysis interval from this borehole splits into four chemostratigraphic units (Figures 6 - 8). The geochemical profiles are also presented (Tables 4 - 6) and expressed

Table 2: Akukwa Ratio Geochemical Profiles.

UNITS	Zr/Cr	Cr/Sc	Zr/La	Sc/Zr	Zn/Sc	TiO_2/K_2O	TiO_2/Zr	Fe_2O_3/MgO	Na_2O/TiO_2	$Log(Zr/Al_2O_3)$
AK 1	**0.2**	**12**	**1.5**	**2**	**1**	**1**	**0.1**	**10**	**3**	**0**
AK 2	0.6	10	2	4	5	1	0.4	4	1	0.4
AK 3	0.7	8	1.5	2	2	1.5	0.1	5	1.2	0.4
AK 4	0.7	8	0.5	12	7	2.5	0.2	25	0.01	0.3

Table 3: Akukwa Trace Element Geochemical Profiles.

UNITS	Zr	Cr	Ba	Cu	La	Ce	Sc	Sr	Y	Zn
AK 1	**15**	**62**	**28**	**12**	**10**	**20**	**5**	**5**	**5**	**5**
AK 2	15	62	50	15	20	80	10	10	20	20
AK 3	35	58	100	20	20	60	10	10	20	20
AK 4	12	140	310	13	50	120	32	32	100	100

below

UNIT AM1

This unit corresponds to the beginning of Well Amansiodo-1 and runs to about 1100m, having high values for MgO, CaO, MnO, P_2O_5, Na_2O, Al_2O_3, Fe_2O_3, TiO_2, K_2O, Cr/Sc, Zn/Sc, Ti_O2/Zr, Na_2O/TiO_2, Zr, Cr, Ba, Cu, La, Ce, Sc, Y and low values for SiO_2, Cr/Sc, Zr/La, Sc/Zr, TiO_2/K_2O, Fe_2O_3/MgO, Log (Zr/Al_2O_3), Sr, Zn. This zone proposes to have been characterised by marine transgression, as shown by high values for MgO, CaO, MnO and P_2O_5. A maximum flooding surface (MFS) suggests around 1000m within the zone.

UNIT AM2

This unit ranges between 1100m to 1400m and has high values for SiO_2, Al_2O_3, Zr/Cr, Cr/Sc, TiO_2/K_2O, Fe_2O_3/MgO, La, Ce and low values for Fe_2O_3, MnO, TiO_2, MgO, CaO, P_2O_5, Na_2O, K_2O, Zr/La, Sc/Zr, Zn/Sc, TiO_2/Zr, Na_2O/TiO_2, Log (Zr/Al_2O_3), Zr, Cr, Ba, Cu, Sc, Sr, Y and Zn. This zone proposes to correspond to regression as seen by high values for SiO_2, Al_2O_3 and low values for CaO and MgO.

UNIT AM3

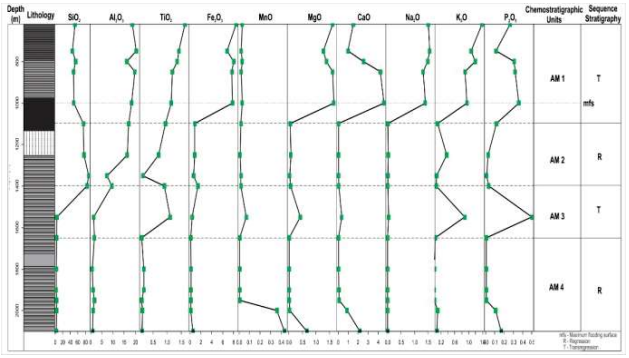

Figure 6: Major Element Geochemical Profiles for Well Amansido-1.

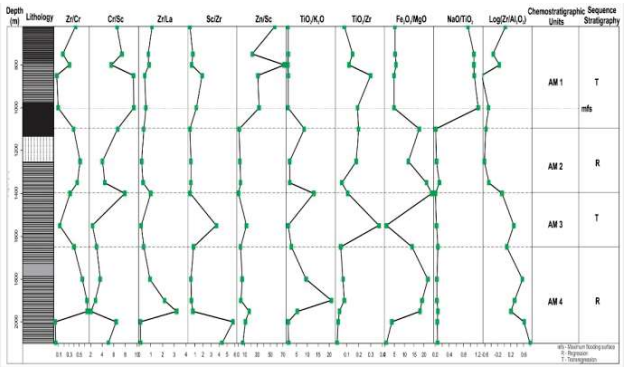

Figure 7: Ratio Geochemical Profiles for Well Amansido-1.

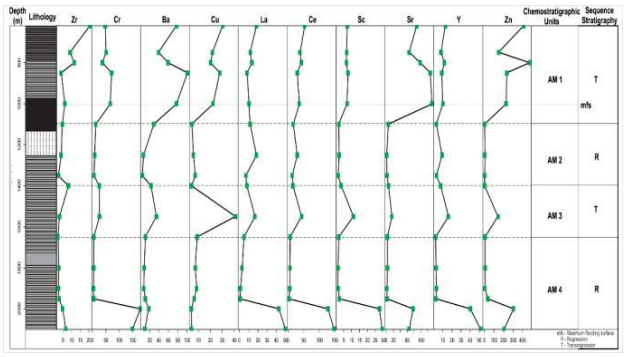

Figure 8: Trace Element Geochemical Profiles Well for Amansido-1.

This range between 1400m to 1700m, and it has high values for MnO, TiO_2, MgO, CaO, K_2O, P_2O_5, Na_2O, Cr/Sc, Zr/La, Sc/Zr, TiO_2/Zr, Fe_2O_3/MgO, Log (Zr/Al_2O_3), Zr, Cr, Ba, Cu, Y and has low values for SiO_2, Fe_2O_3, Al_2O_3, Zr/Cr, TiO_2/K_2O, Zn/Sc, Na_2O/TiO_2, La, Ce, Sc, Sr, and Zn. This zone is proposed to be characterized by the transgression of the marine as seen by high values for MnO, MgO, CaO and low values for SiO_2, Al_2O_3.

UNIT AM4

This begins from about 1700m and runs down the well. It has high values for MnO, MgO, CaO, P_2O_5, Zr/Cr, Cr/Sc, Zr/La, Sc/Zr, Zn/Sc, TiO2/K_2O, Fe_2O_3/MgO, Log (Zr/Al_2O_3), Ba, Cu, La, Ce and low values for SiO_2, Al_2O_3, Fe_2O_3, TiO_2, K_2O, Na_2O, TiO_2/Zr, Na_2O/TiO_2, Zr, Cr, Sc, Sr, Y and Zn. The zone is suggested to have been characterized by marine regression as shown by the various values for major, trace and ratios analyzed.

SALINITY CONDITIONS

Sr/Ba- Strontium (Sr) and Barium (Ba) are alkaline earth metals with chemically similar properties. Sr content in seawater is often high, so it is possible to use Sr/Ba ratios to discriminate against freshwater (Sr/Ba: < 1) and marine sediments (Sr/Ba: > 1) (Sun *et al*., 1997). For example, Sr/Ba ratios between 1.0 and 0.5 suggest brackish water. Conversely, a Sr/Ba ratio above 1.0 in lacustrine

Table 4: Amansiodo Major Element Geochemical Profiles.

UNITS	SiO_2	Al_2O_3	TiO_2	Fe_2O_3	MnO	MgO	CaO	Na_2O	K_2O	P_2O_5
AM 1	60	20	1.5	8	0.02	1.7	5	1.5	1.8	0.4
AM 2	82	17	1	2	0.02	0.2	0	0	0.4	0.1
AM 3	5	3	1.2	1	0.1	0.5	1	0	1	0.5
AM 4	5	3	0.1	1	0.02	0.6	2	0	0	0.2

Table 5: Amansiodo Ratio Geochemical Profiles

UNITS	Zr/Cr	Cr/Sc	Zr/La	Sc/Zr	Zn/Sc	TiO_2/K_2O	TiO_2/Zr	Fe_2O_3/MgO	Na_2O/TiO_2	Log(Zr/Al_2O_3)
AM 1	0.4	10	1	2	70	1	0.3	5	1.2	0.2
AM 2	0.6	4	0	1	7	2	0.2	20	0.1	-0.6
AM 3	0.2	2	0	4	10	20	0.4	0	0	0.4
AM 4	0.6	6	3	6	12	0	0.1	25	0.1	0.7

Table 6: Amansiodo Trace Element Geochemical Profiles.

UNITS	Zr	Cr	Ba	Cu	La	Ce	Sc	Sr	Y	Zn
AM 1	20	50	100	30	10	50	10	140	10	500
AM 2	5	20	20	10	20	25	5	10	10	0
AM 3	6	30	40	40	20	50	15	20	20	150
AM 4	6	200	20	10	50	150	30	80	50	300

environments under an arid climate can indicate saline lake water (Shi *et. al.*, 2003; Meng *et. al.*, 2012).

The Sr/B ratios in Akukwa-2 range from 0.21 to 0.63 (Figure 9{e}), promoting a fresh-brackish water climate. The Sr/Ba ratios in the Amansiodo-1 range from 0.22 to 1.29 (average 0.53), indicating alternating freshwater and saline conditions. High Sr/Ba ratios often correspond to high Sr/Cu values (see Figures 9{b} & 10{b}), which indicates that increases in salinity between the two wells may have been caused by climate change.

B and B/Ga-Boron (B) and gallium (Ga) have slightly different chemical properties. Boron is a mobile variable in water, and its content increases with salinity (Deng & Qian, 1993), while Ga is a more immobile element. Liu *et. al.* (1984) found that the content of Ga is higher in continental freshwater mudstones (20-35 ppm) than in marine rocks (7-10 ppm). Therefore, as additional salinity proxies, B and B/Ga can also be used. In freshwater lakes, B is below 60µg/g and B/Ga is below 3-3.3, while in salt water, B and B/Ga surpass 100 µg/g and 4.5-5.0, respectively (Wang *et. al.,* 1979; Deng & Qian, 1993).
The B content as well as Akukwa-2 B/Ga ratios (33.1-57.9 µg/g; 1.30-2.89) and Amansiodo-1 ratios (19.2-86.7 µg/g; 1.09-35.22; Figures 9 & 10{c,f}), reflects temporary brackish water conditions.

REDOX PROXIES

V/Cr, Ni/Co, V/(V+Ni), Cu/Zn, (Cu+Mo)/Zn, and trace elements such as V, Ni, Mn, and Mo are sensitive redox proxies (Arthur *et. al.,* 1994; Anderson *et. al.*, 1989; Morford & Emerson,1999). For anoxic conditions, vanadium is enriched more than nickel (Lewan *et. al.,* 1982). Generally, V/(V+Ni) ratios greater than 0.60 reflect anoxia, suboxic conditions reflect between 0.46 and 0.60,

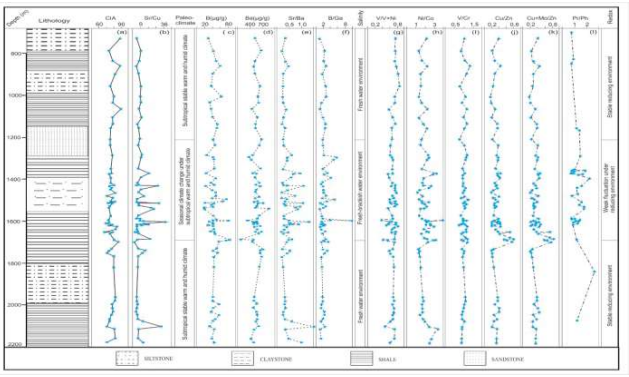

Figure 9: Vertical distribution of some geochemical proxies for paleoenvironment and paleoclimatic interpretation for Akukwa-2 after Strobel *et. al.,* 2015.

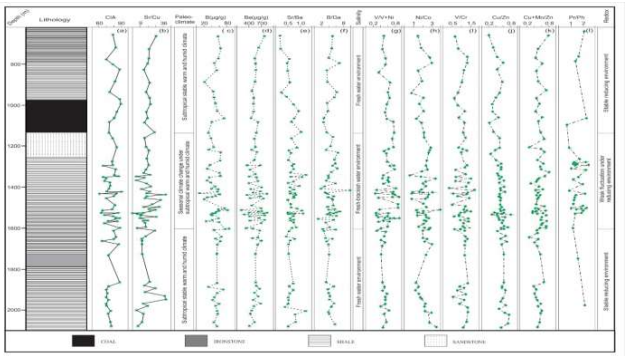

Figure 10: Vertical distribution of some geochemical proxies for paleoenvironment and paleoclimatic interpretation for Amansiodo-1 after Strobel *et. al.,* 2015.

and oxic environments reflect less than 0.46 (Teng *et. al.*, 2005; Wang, 2003). V/(V+Ni) ratios of Akukwa-2 shale range from (0.39 to 0.45, with an average of 0.42, while the one from Amansiodo-1 ranges from 0.40 to 0.88 with an average of 0.45 (Figures 9 & 10{g}), suggesting oxic deposition.

Cu/Zn, V/Cr, Ni/Co, and (Cu+Mo)/Zn ratios increased with the declining availability of oxygen (Wang, 2003) and were used as additional redox indicators. Figures 9 –&10 {h-k} show the vertical variance of the ratios of the given variable. All ratios in the Akukwa-2 and Amansiodo-1 are well relatively uniform. However, in Akukwa-2 (V/Cr: 1.04; Cu/Zn: 0.37; Ni/Co: 2.49; (Cu+Mo)/Zn: 0.39), the mean ratios are slightly higher than in Amansiodo-1 (V/Cr: 0.97; Cu/Zn: 0.34; Ni/Co: 2.31, (Cu+Mo)/Zn: 0.37).

Trace element ratios (Th/U, V/Cr, Ni/Co, and V/(V+Ni)) may contain information about paleoredox conditions (Jones & Manning, 1994; Hatch & Leventhal, 1992; Rimmer *et. al.,* 2004). Under oxic conditions, Thorium is generally concentrated in clay sediments (Wignall &

Myers, 1988; Adams & Weaver, 1958). Under organic matter-rich reducing conditions, sediments can trap aqueous U (Holland, 1984; Kochenov *et. al.,* 1977). Therefore, small Th/U ratios are characteristic of anoxic conditions with high authentic U. As an indicator of oxic sediments, Th/Ub< 2 has been commonly used (Wignall & Twitchett, 1996). Nickel and V are concealed in organic matter under anoxic conditions (Breit & Wanty, 1991; Lewan & Maynard, 1982). In contrast, redox conditions do not affect Co and Cr concentrations linked to detrital components (Ross & Bustin, 2006). Thus high values of V/Cr, Ni/Co and V/(V+Ni) reflect oxic conditions (Jones & Manning, 1994). A clear interpretation of paleoredox conditions in the Akukwa-2 and Amansiodo-1 shale samples using standards for Th/U, Ni/Co and V/Cr (Figures 11 - 12). However, the Akukwa-2 and Amansiodo-1 shale ratios of V/(V + Ni) range from 0.62 to 0.88, pointing at all in oxic conditions, while other proxies also indicate dysoxic to oxic conditions (Figures 11 - 12).

Rhenium, due to its low detrital concentrations, is a valuable resource for evaluating redox conditions (0.5 ppb in continental crust; Crusius *et. al.,* 1996) and is not linked to Fe or Mn cycling (Crusius *et. al.*, 1996), usually acting in oxic and anoxic conditions as a conservative item. Redox activity is, therefore, simplistic and useful to track accurate accumulation (through diffusive sediment flux; Morford *et. al.,* 2001). It has been proposed that rhenium may be introduced into sulfides after spreading through the sediment-water interface (Colodner *et. al.,* 1993). Re/Mo ratios are used (Crusius *et. al.,* 1996) to distinguish suboxic sedimentation. High Re/Mo ratios (> 15 x 10-3) are suggestive of suboxic conditions as Re over Mo is preferentially enriched in low-sulfide environments (Crusius *et. al.,* 1996). In contrast, anoxic/sulfidic groundwater has lower Re/Mo ratios, closer to the modern marine-water value of 15 x 10-3. Sediments of Akukwa-2 and Amansodo-1 plot below the seawater Re/Mo (Figure 13), indicating suboxic deposition with occasional anoxic conditions.

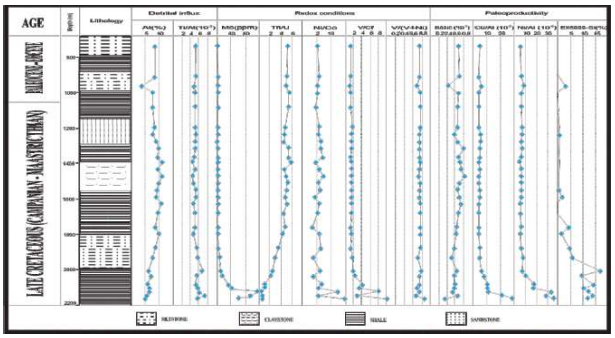

Figure 11: Stratigraphic distribution of detrital influx proxies (Al, Ti/Al), redox proxies (Mo, Th/U, Ni/Co,V/Cr and V/(V+Ni) and Paleoproductivity proxies (Babio, Cu/Al, Ni/Al) in Well Akukwa-2.

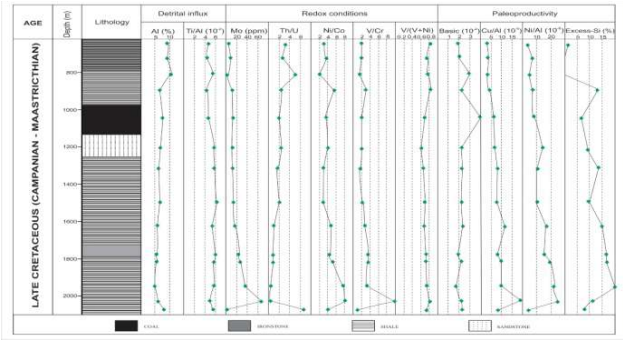

Figure 12: Stratigraphic distribution of detrital influx proxies (Al, Ti/Al), redox proxies (Mo, Th/U, Ni/Co,V/Cr and V/(V+Ni) and Paleoproductivity proxies (Babio, Cu/Al, Ni/Al) in Well Amansiodo-1.

DETRITAL INFLUX PROXIES

The contents of titanium, aluminium, Silicon, Zircon, and Thorium were widely used as indicators of detrital influx (Tribovillard *et. al.,* 2006; Murphy *et. al.,* 2000). Aluminum is the prominent conservative in a fine-grain deposition for the detrital aluminosilicate component (Arthur *et. al.,* 1985; Calvert & Pedersen, 2007; Arthur & Dean, 1991). In this paper, Al concentrations are generally high in the shale (Figures 11- 12), indicating a rise in detrital clay influx. Titanium is commonly found in clays and heavy minerals such as rutile, while Si is found in detrital and biogenic components (Kidder & Erwin, 2001). In various prior studies, the Si/Al ratio was used as a detrital influx proxy, reflecting the quartz-to-clay ratio (Rimmer *et. al.,* 2004; Murphy *et. al.,* 2000). However, the silica or Si/Al ratios may be an inaccurate indicator of detrital influx since biogenic silica could theoretically originate from radiolarians in siliceous and silty shale (Rimmer *et. al.,* 2004; Schieber *et. al.,* 2000). The relative distribution of Ti/Al for all samples in this study indicates a very homogeneous supply of coarse-grain detrital fractions in the shale of Akukwa-2 and Amansiodo-1 (Figures 11 - 12).

PALEOPRODUCTIVITY PROXIES

Barium is known as a paleoproductive proxy because the biogenic barite is associated with the decay of phytoplankton (Francois e*t. al.,* 1995; Dymond *et. al.,* 1992; Monnin *et. al.,* 1999; Jeandel *et. al.,* 2000). Biogenic Ba (Babio) has been demonstrated in the water column as an indicator for the measurement of carbon emissions from the photon zone and is considered a valid proxy for paleoproductivity (Tribovillard *et. al.,* 1996; Brumsack, 1989; Martinez-Ruiz *et. al.,* 2000; McManus *et. al.,* 1998a, 1998b, 1999; Joachimski *et. al.,* 2002; Eagle *et. al.,* 2003; Tribovillard *et. al.,* 2004; Averyt & Paytan, 2004; Riquier *et. al.,* 2005; Joachimski *et. al.,* 2002). The formula used to assess Ba_{bio} content is:

$Ba_{bio} = Ba_{tot} - (Al_{tot} \times Ba/Al_{alu}) = Ba_{tot} - (Al_{tot} \times 0.0075)$

Whereas Ba_{bio}: is the content of biogenic Ba, Ba_{tot} is the Total content of Ba, Ba/Al_{alu}: is the Ba/Al ratios of

aluminosilicate detritus in crustal rocks, and Al_{tot}: is the total Al content. It means that all of Al is from aluminosilicate in sediments. The aluminosilicate factor Ba/Al_{alu} ratios range from 0.005 to 0.01 in crustal rocks (Taylor, 1964), and the value of 0.0075 are commonly used to measure the Ba_{bio} content (Dymond *et. al.,* 1992). In both Akukwa-2 and Amansiodo-1, the batot and ba_{bio} are high. In sulfate reduction conditions (organic-rich shale), however, barite may dissolve, and Ba may migrate to pore water, which may make Ba_{bio} and Ba_{tot} an accurate predictor of paleoproductivity in organic-rich sediments formed under these conditions (Torres *et. al.,* 1996; Van Os *et. al.*, 1991; Van Santvoort *et. al.,* 1996). Hence the high concentrations of Batot and Ba_{bio} in high organic-rich shale of Akukwa-2 and Amansiodo-1 suggest a higher paleoproduction.

Most deposited as organometallic complexes are Nickel and Cu. Ni and Cu released during the decay of organic matter can be incorporated into pyrite under sulfate reduction conditions (Algeo & Maynard, 2004; Fernex *et. al.,* 1992; Piper & Perkins, 2004). Although the sedimentary organic matter deteriorated after deposition, Ni and Cu could point to its vital presence. Hence Ni and Cu can be used as accurate measures of Productivity. The ratios Cu/Al and Ni/Al indicate the standardised patterns at both wells supporting the high paleoproductivity. In addition, due to precipitating authentic quartz form dissolution and recrystallisation by radiolarians, excess silica concentrations are due to radiolarians, and their content (excess silica) may imply paleoproductivity (Schieber, 1996). The excess content of silica reveals similar patterns to the Cu/Al and Ni/Al ratios (Figures 11 - 12).

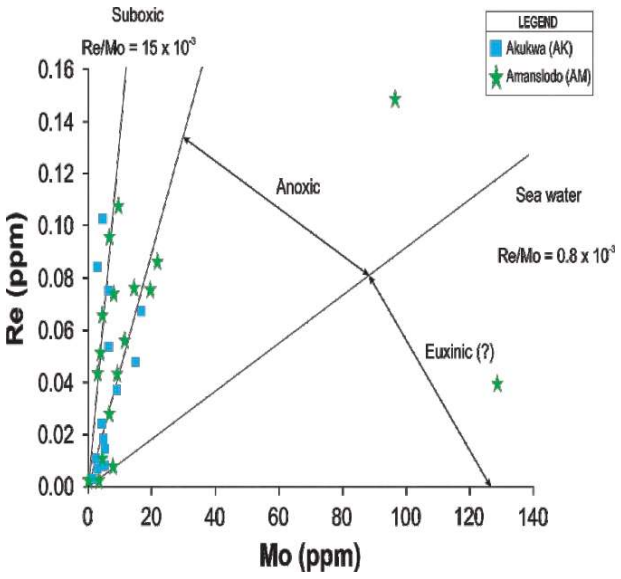

Figure 13: Rhenium vs. Mo ratio used for identifying anoxic and dysonic sedimentation modified after Crusius *et. al.,* 1996.

MINERALOGY

Clay minerals are of great importance among the most valuable and useful industrial minerals in the world. They are used in a variety of geological applications, such as stratigraphic correlations, deposition environment indicators and hydrocarbon generation temperature indicators. X-ray diffraction (XRD) technique is widely used to identify whole rock mineralogy and clay mineralogy through interaction of the x-ray beam with a sample. The quantitative analysis of clay minerals in soils involves working out of peak intensity (area or height) ratios based on standard powder diffraction of the International Powder Diffraction File. In this research, using x-ray diffraction (XRD) patterns following the Brown and Brindley (1984) method, the identification of the specific shale mineralogical composition was obtained.

MINERALOGICAL COMPOSITION

Identification of whole rock mineralogy of rocks and sediments has been widely attempted with an application of x-ray diffraction (XRD) technique. In this research, identification of the mineralogical composition of the studied shale samples were also attempted using x-ray diffraction (XRD) method and both qualitative (Peak patterns) and quantitative results of all whole-rock samples are presented in Table 7 and 8. Generally, the results indicate presence of clay and non-clay minerals for both Akukwa and Amansiodo wells with kaolinite as the predominant among the clay minerals whereas quartz as the most abundant among the non-clay types and also carbonate and iron minerals are also present in minor compositions.

AKUKWA WELL (AK)

The analyzed shale samples are composed of non-clay, clay, evaporites, carbonate and minor iron minerals. The non-clay rock forming minerals includes quartz, microcline, anatase, plagioclase, jarosite and muscovite whereas the clay minerals present are kaolinite, smectite and palygorskite in the decreasing order with the kaolinite having the highest composition whereas palygorskite have lowest. Also, it is interesting to note that aside the clay and non-clay rock forming minerals, chemical minerals (evaporite) including gypsum, halite and chlorite, carbonate (calcite) and iron rich mineral (pyrite) are also present though, in fewer samples Table 7 (Figure 14 and 15).

Generally, the minerals present in the samples show 3 categories of behavior. Category 1 consists of minerals like quartz, microcline, kaolinite and pyrite that are present throughout from the upper through the middle to the lower parts of the well. Minerals such as anatase, plagioclase, kaolinite, gypsum, jarosite and chlorite are present in category 2. Meanwhile, in the category 3, minerals including muscovite, smectite, palygorskite, calcite, halite and chlorite are present. Interestingly, it is observed that there is significant reduction in the quantity of Kaolinite

from category 2 as chlorine started to show in the shale samples and this goes on down to category 3.

Table 7: Mineralogical composition of the Shale samples from Akukwa well.

Weight%	AK1	AK3	AK5	AK7	AK9	AK11	AK13	AK15	AK17	AK19
Quartz	40.54	26.36	33.53	28.51	19.98	85.92	3.1	5.95	5.52	10.93
Gypsum	1.97	2.49	1.68	4.85	0.00	0.00	6.41	0.00	0.00	4.97
Jarosite	0.00	14.45	10.53	0.00	0.00	0.00	15.42	0.00	0.00	6.26
Kaolinite	35.94	40.37	36.34	39.85	10.61	0.00	0.00	4.75	6.34	4.39
Microcline	8.36	6.2	7.45	5.92	1.65	9.56	6.41	2.59	5.63	2.12
Anatase	3.24	4.13	3.35	3.73	1.39	0.00	0.00	0.00	0.00	1.16
Smectite	0.00	0.00	0.00	0.00	53.73	0.00	0.00	67.74	53.88	70.17
Muscovite	0.00	0.00	0.00	0.00	0.00	1.77	8.16	0.00	0.00	0.00
Plagioclase	4.09	1.67	2.09	1.43	1.55	2.74	0.00	0.00	0.00	0.00
Pyrite	5.86	4.33	5.03	6.91	3.73	0.00	1.03	1.07	1.15	0.00
Calcite	0.00	0.00	0.00	8.8	6.22	0.00	0.00	7.29	7.94	0.00
Halite	0.00	0.00	0.00	0.00	1.13	0.00	1.59	1.86	0.00	0.00
Chlorite	0.00	0.00	0.00	0.00	0.00	0.00	10.48	12.51	11.82	15.18
Palygorskite	0.00	0.00	0.00	0.00	0.00	0.00	48.98	10.6	19.55	0.00

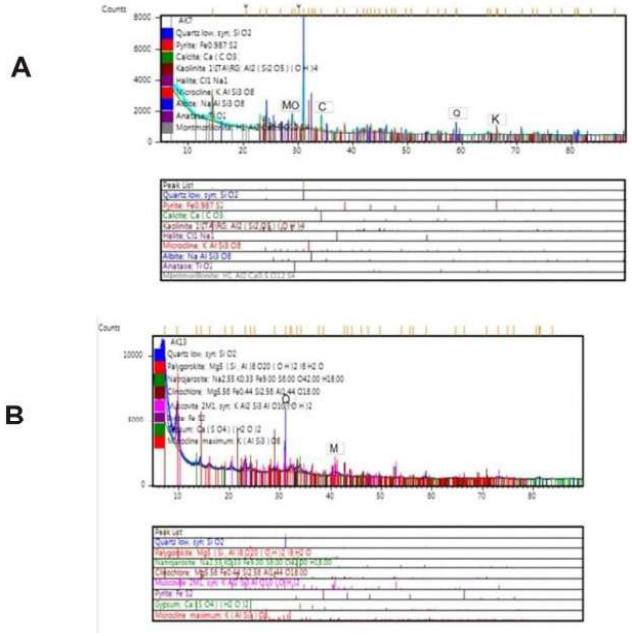

Figure 14: (A): Diffractograms of the Clay (sample AK 7) from Akukwa Well. (Mo- Montmorillonite, C- calcite, Q- Quartz, K-Kaolinite. (B): Diffractogram of the Clay (sample AK 13) from Akukwa Well. (M-Muscovite Q-Quartz).

AMANSIODO WELL (AM)

The analyzed shale samples from Amansiodo well are also composed of non-clay, clay, evaporites, carbonate and iron minerals like in the Akukwa well (Table 8 and Figure 16 and 17). It is noted that non-clay rock forming minerals (e.g. quartz, microcline, anatase, plagioclase, jarosite, muscovite, covellite and rutile) occur in various proportions with quartz having the highest proportion.

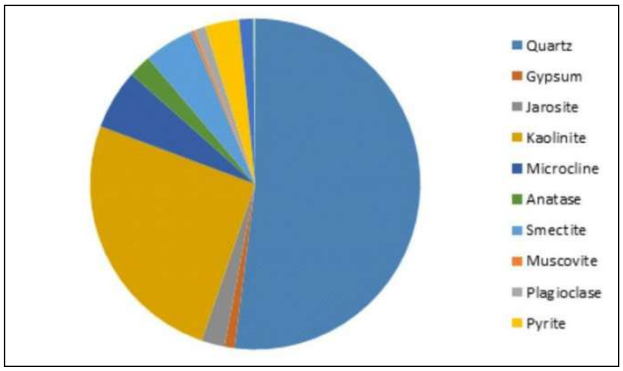

Figure 15: Pie Chart showing the mineralogical compositions of studied Shale from Akukwa well.

Among the clay minerals, kaolinite has the highest percentage while smectite occur only in a sample (50.72) and in higher proportion. It is interesting to note that palygorskite is absent in all the analyzed samples from the well. It is also interesting to note that unlike Akukwa well, the minerals present here are only gypsum and chlorite whereas halite is absent. Aragonite is also present alongside with calcite among the carbonate minerals while the iron rich minerals are composed of pyrite and hematite.

Same behavioral pattern is also noted among the minerals present in this well with 3 categories delineated though, with little difference. Minerals present in category 1 include quartz, kaolinite and pyrite that are present in all the analyzed samples from the lower through the middle to the upper parts of the well. Minerals present in category 2 includes microcline, anatase and plagioclase) present in the samples found in the lower and upper parts of the well whereas, other minerals that made up of the category 3 only appears from middle to the lower part of the well. It is interesting to note that unlike the Akukwa well, muscovite was found only in a sample (AM1) that is closer to the upper (surface) part of the Amansiodo well.

DIAGENESIS, PALEOCLIMATE AND PALEOENVIRONMENTS OF AKUKWA AND AMANSIODO WELL

Mineralogical compositions of the studied samples are employed here for deposition environment reconstruction. The mineralogical composition of sediments can be used to determining its depositional environments according to Mamman *et. al.* (2010). There are two main environments recognized within the two wells using the mineralogical composition and their abundance, especially kaolinite and chlorite. Generally, presence and abundance of rock forming minerals including quartz, microcline, kaolinite and pyrite that are present mostly in the upper parts of the well indicating continental environments. In contrast, minerals including muscovite, smectite, palygorskite, calcite, halite and chlorite with a significant decrease in kaolinite while

chlorite start increasing. This may suggest a change in environments from continental to marine. Also, an increase in the abundance of siderite and pyrite contents may reflects a different climate because ferric minerals were formed in a warm, humid, non-oxidizing environment in the basin as more reducing conditions become gradually evident with depth.

Table 8: Mineralogical composition of the samples from the Amasiodo Well.

Weight%	AM1	AM3	AM5	AM7	AM8	AM9	AM12	AM13	AM15	AM16	AM17
Quartz	72.21	63.06	63.9	42.93	86.38	94.55	46.02	56.72	16.13	38.85	38.85
Gypsum	2.53	0.00	1.72	1.32	0.00	0.00	1.66	0.00	4.05	2.19	2.19
Jarosite	0.00	0.00	0.00	0.00	0.00	0.00	15.84	0.00	10.08	0.00	0.00
Kaolinite	15.27	18.87	23	41.24	13.62	4.38	26.7	26.9	13.15	16.23	14.13
Microcline	7.36	9.31	9.01	9.2	0.00	0.00	6.2	5.64	0.00	9.93	9.93
Anatase	1.41	1.94	2.26	3.14	0.00	0.00	0.00	0.00	1.56	3.37	3.37
Smectite	0.00	0.00	0.00	0.00	0.00	0.00	0.00	0.00	50.72	0.00	0.00
Muscovite	3.74	0.00	0.00	0.00	0.00	0.00	0.00	0.00	0.00	0.00	0.00
Plagioclase	0.00	1.35	0.00	0.00	0.00	0.00	3.58	3.82	0.00	4.03	4.03
Pyrite	0.00	5.47	1.82	3.49	0.00	1.48	0.00	4.6	1.02	5.4	5.4
Calcite	0.00	0.00	0.00	0.00	0.00	7.56	0.00	2.32	0.00	0.00	0.00
Halite	1.24	0.00	1.33	0.00	0.00	0.00	1.24	1.41	1.36	0.00	0.00
Chlorite	0.00	0.00	0.00	0.00	0.00	7.02	10.85	12.38	3.28	16.43	0.00
Aragonite	0.00	0.00	0.00	0.00	0.00	30.37	0.00	0.00	0.00	0.00	0.00
Covellite	0.00	0.00	0.00	0.00	0.00	2.29	0.00	0.00	0.00	0.00	0.00
Rutile	0.00	0.00	0.00	0.00	0.00	1.68	0.00	0.00	0.00	0.00	0.00
Hematite	0.00	0.00	0.00	0.00	0.00	1.08	0.00	0.00	0.00	0.00	0.00

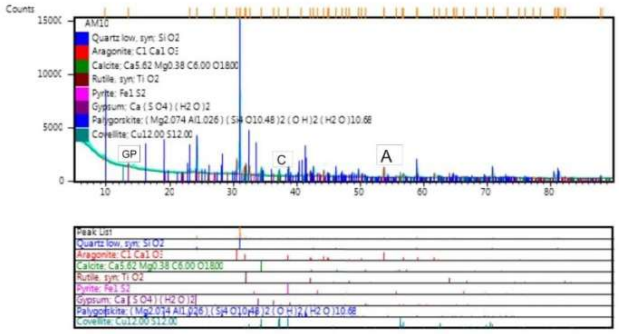

Figure 16: Diffractogram of the Clay (sample AM10 showing the non-clay mineral peaks) from Amasiodo well. (GP- Gypsum-, C- calcite, A-Aragonite).

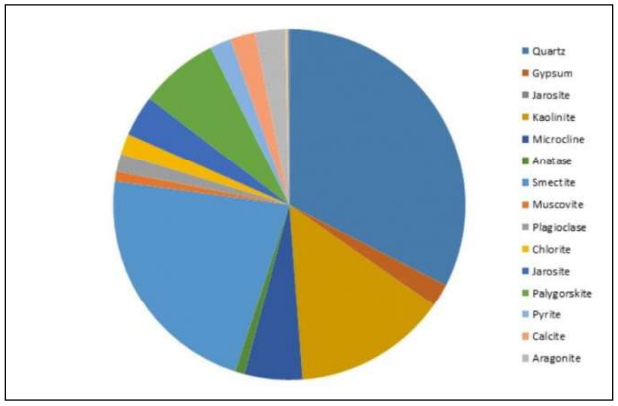

Figure 17: Pie Chart showing the mineralogical compositions of studied Shale from Amasiodo well.

DIAGENESIS

Presence of calcite suggest a limited carbonate remobilisation during diagenesis. Presence of diagenetic clay minerals including smectite which is inferred to be a product of kaolinite transformation during deep burial whereas chlorites concentrations which is typically locally augmented in the lower parts is suggested to be a product of transformation of smectitic clay or of precipitation from more alkaline pore water points deposition with the prevalence of humid conditions. In order to produce both gypsum and anhydrite, the diagenetic solution-precipitation process of halite and chlorite can indicate syn-depositional and early diagenetic development. Early diagenetic processes occur, according to Shearman (1983), after the gypsum has been precipitated, but before it has been substantially buried. According to Hussain (1989), the transformation from gypsum to anhydrite by solution-reprecipitation is often characterized by chicken-wire textures (Schreiber, 1988). Gypsum may precipitate in the form of nodules on layers already rich in gypsum. Meanwhile the dissolved carbonate mud is crystallized by anhydrite and other initial impurities are forced out and form a layer around the anhydrite nodules. The dark gypsum and anhydrite are thought to be from carbonate substitution. In the Akukwa and Amansiodo wells, gypsum and halite are found at varying depths (Figure 18).

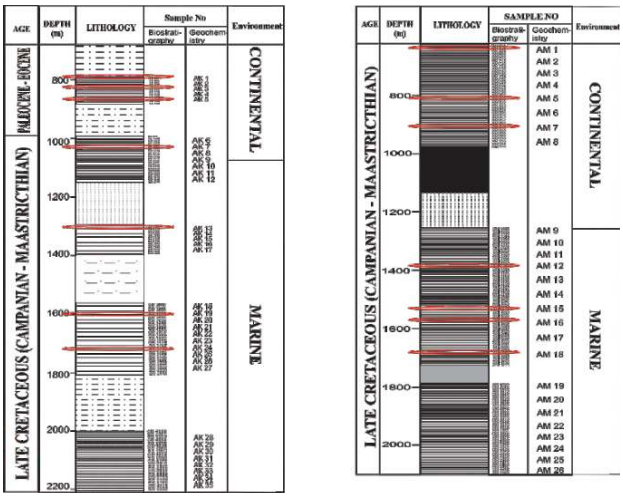

Figure 18: The occurrence of gypsum and halite within the Akukwa and Amansiodo Wells. Note: The red circles indicate the intervals where the evaporates occur.

There is an appearance of metastable aragonite which has ability to transforms to calcite at depth of about 1,200 to 1,300m which suddenly disappearance and absent in other samples in lower part of the section. Siderite and pyrite are also noted to be increasing as the calcite are increasing with depth. According to Deans (1934), ferric oxides are prone to conversion to soluble ferrous iron in the strongly reducing environment. Also, according to Ryo and Azuma

(1981), an increase in the activity of iron promotes extensive precipitation of siderite, and with the appearance and increase of calcite at burial depths above 1,000 m strongly reflect the original depositional environments. This may reflect climatic controls based on palynological studies with the presence of aragonite.

CONCLUSIONS

In the wells Akukwa-2 and Amansiodo-1, four chemostratigraphic units, namely AK1, AK2, AK3, AK4, AM1, AM2, AM3 and AM4, were identified. The elemental composition of the zones reflects alternating marine transgression and regression down holes. In the Akukwa-2, the Sr/Ba ratios range from 0.21 to 0.63, supporting a freshwater condition, while the Sr/Ba ratios in the Amansiodo-1 range from 0.22 to 1.29 (average 0.53), suggesting alternating freshwater and brackish water conditions. The B content and the ratios of Akukwa-2's B/Ga (33.1-57.9 μg/g; 1.30-2.89) and Amansiodo-1 (19.2-86.7 μg/g; 1.09-35.22) reflect temporary brackish water conditions. The distribution of Ti/Al in this study for all samples suggests a rather homogeneous supply of coarse-grain detrital fractions in Akukwa-2 and Amansiodo-1 shale.

V/(V+Ni), Ni/Co, V/Cr, Cu/Zn, Th/U, Re/Mo ratios and (Cu+Mo)/Zn indicate mainly oxic condition and slight fluctuation in suboxic and dysoxic for the investigated shale. Redox proxies show that the shale was deposited under fairly oxic conditions controlled by high paleoproductivity, moderate-high detrital influx, and dysoxic/oxic conditions during their accumulation.

Mineralogy reveals that the shales are rich in clay, non-clay, evaporites, carbonate and iron minerals. There is enrichment of kaolinite and quartz in the upper intervals of the wells suggesting more continental conditions whereas the lower part is enriched in chlorite but depleted kaolinite indicating seaward contributions. Gypsum and halite occurred in few intervals in the wells suggesting occasional evaporate diagenetic environment and dry conditions. Based on the values of CIA, PIA and CIW ranging from 84% to 93%, it can be suggested that the litho components of the shales were subject to intense chemical weathering which were substantiated by several binary and ternary plots such as Na_2O, K_2O, CaO and PIA. Also, in the diagram K_2O/Na_2O vs. PIA, (K_2O+Na_2O) vs. PIA, MgO vs. CIA, A-CN-K, A-CNK-FM.

REFERENCES CITED

Adams, J.A.S., and C.E. Weaver, (1958). Thorium to uranium ratios as indicators of sedimentary processes: examples of the concept of geochemical facies: America Association of Petroleum Geology Bulletin, v. 42, p. 387–430.

Akande, S.O. and B.D. Erdtmann, (1998). Burial Metamorphism (Thermal Maturation) in Cretaceous Sediments of the southern Benue Trough and Anambra Basin, Nigeria. American Association of Petroleum Geologists Bulletin. v. 82, p. 1191

Akande, S.O., I.B. Ogunmoyero, H.I. Petersen, and H.P. Nytoft, 2007, Source Rock Evaluation of Coals from the Lower Maastrichtian Mamu Formation, S.E. Nigeria: Journal of Petroleum Geology, vol. 30, p. 303-324.

Algeo, T.J., and J.B. Maynard, (2004). Trace-element behaviour and redox facies in core shales of Upper Pennsylvanian Kansas-type cyclothems: Chemical Geology, v. 206, p. 289–318.

Anderson, R.F., M.Q. Fleisher, and A.P. LeHuray, 1989, Concentration, oxidation state and particulate flux of uranium in the Black Sea: Geochimica et Cosmochimica Acta, v. 53, p. 2215–2224. https://doi.org/10.1016/0016-7037(89)90345-1

Arthur, M.A. and B.B. Sageman, (1994). Marine black shales: Depositional mechanism and environments of ancient deposits: Annual Review of Earth and Planetary Science, v. 22, p. 499- 551. https://doi.org/10.1146/annurev.ea.22.050194.002435

Arthur, M.A., and W.E. Dean, (1991). A holistic geochemical approach to cyclo mania-examples from Cretaceous pelagic limestone sequences. In: Einsele, G., Ricken,W., Seilacher, A. (Eds.), Cycles and Events in Stratigraphy: Springer-Verlag, Berlin, p. 126–166.

Arthur, M.A., W.E. Dean, R.M. Pollastro, G.E. Claypool, and P.A. Scholle, (1985). Comparative geochemical and mineralogical studies of two cyclic transgressive pelagic limestone units, Cretaceous Western Interior Basin, U.S. In Pratt, L.M., Kauffman, E.G., Zelt, F.B. (Eds.), Fine-grained Deposits and Biofacies of the Western Interior Seaway: Evidence of Cyclic Sedimentary Processes, Society of Economic Paleontologists and Mineralogists, 1985 Midyear Meeting, Golden, Colorado: Field Trip Guidebook, no. 4, p. 16–27.

Averyt, K.B., and B. Paytan, (2004). A comparison of multiple proxies for export production in the equatorial Pacific: Paleoceanography, v. 19, p. 4003–4016.

Bown, G. and G.W. Brindley, (1984), Crystal Structures of Clay Minerals and Their X-Ray Identification. 2nd Edition: Mineralogical Society, London, p. 305-360.

Breit, G.N., and R.B. Wanty, (1991). Vanadium accumulation in carbonaceous rocks: a review of geochemical controls during deposition and diagenesis: Chemical Geology, v. 91, p. 83–97.

Brumsack, H.J., (1989). Geochemistry of recent TOC-rich sediments from the Gulf of California and the Black Sea: Geologische Rundschau, v. 78, p. 851–882.

Calvert, S.E., and T.F. Pedersen, (2007). Elemental proxies for palaeoclimatic and palaeoceanographic variability in marine sediments: Interpretation and Application. In: Hillaire-Marcel, C., de Vernal, A. (Eds.), Paleoceanography of the Late Cenozoic. Methods in Late Cenozoic Paleoceanography Vol. Part 1: Elsevier, New York, p 567–644.

Colodner, D., J. Sachs, G. Ravizza, K. Turekian, J. Edmont, and E. Boyle, (1993). The geochemical cycle of rhenium: a reconnaissance: Earth and Planetary Science Letters, v. 117, p. 202–221.

Crusius, J., S. Calvert, T. Pedersen, and D. Sage, (1996). Rhenium and molybdenum enrichments in sediments as indicators of oxic, suboxic, and sulfidic conditions of deposition: Earth Planet. Science Letter, v. 145, p. 65–78.

Das, N., (1997). Chemostratigraphy of sedimentary sequences: A review of state of the art: Journal of Geological Society of India, v. 49, p. 621–628.

Deans, T. (1934). The Spherulitic Ironstones of West Yorkshire. Geological Magazine, 71(2), 49–65. doi:10.1017/S0016756800092803

Deng, H.W. and K. Qian, (1993). Sedimentary geochemistry and environment analysis. Lanzhou in China: Gansu Science and Technology Press, Gansu, China, p. 1-150.

Dymond, J., E. Suess, and M. Lyle, (1992). Barium in deep-sea sediments: a geochemical proxy for paleoproductivity: Paleoceanography, v. 7, p. 163–181.

Eagle, M., A. Paytan, K.R. Arrigo, G. van Dijken, and R.W. Murray, (2003). A comparison between excess barium and barite as indicators of carbon export: Paleoceanography, v. 18, p. 2101–2113.

Fairhead, J.D. and C.S. Okereke (1987). A Regional Gravity Study of the West African Rift System in Nigeria and Cameroon and its Tectonic Interpretation: Tectonophysics, v. 143, p. 141-159.

Fernex, F., G. Février, J. Benaïm, and A. Arnoux, (1992). Copper, lead and zinc trapping in Mediterranean deep-sea sediments: probable coprecipitation with manganese and iron: Chemical Geology, v. 98, p. 293–308.

Francois, R., S. Honjo, S.J. Manganini, and G.E. Ravizza, (1995). Biogenic barium fluxes to the deep sea: implications for paleoproductivity reconstruction: Global Biogeochemical Cycle, v. 9, no. 2, p. 289–303.

Genik, G.J., (1992). Regional Framework, Structural and Petroleum Aspects of Rift Basins in Niger, Chad and Central African Republic (C.A.R.): Tectonophysics, v. 213, p. 169–185. http://dx.doi.org/10.1016/0040-1951(92)90257-7

Hatch, J.R., and Leventhal, J.S., (1992). Relationship between inferred redox potential of the depositional environment and geochemistry of the Upper Pennsylvanian (Missourian) stark shale member of the Dennis Limestone, Wabaunsee County, Kansas, USA: Chemical Geology, v. 99, p. 65–82

Holland, H.D., (1984). The Chemical Evolution of the Atmosphere and Oceans: Princeton University Press, 287p.

Hussain, M., and J.K. Warren, (1989), Nodular and enterolithic gypsum; the "sabkha-tization" of salt Flat Playa, West Texas: Sedimentary Geology, v. 64, p. 13-24.

Jeandel, C., K. Tachikawa, A. Bory, and F. Dehairs, (2000). Biogenic barium in suspended and trapped material as a tracer of export production in tropical NE Atlantic (EUMELI sites): Marine Chemistry, v. 71, p. 125–142.

Joachimski, M.M., R.D. Pancost, K.H. Freeman, C. Ostertag-Henning, and W. Buggisch, (2002). Carbon isotope geochemistry of the Frasnian–Famennian transition: Palaeogeography, Palaeoclimatology and Palaeoecology, v. 181, p. 91–109.

Jones, B., and D.A.C. Manning, (1994). Comparison of geochemical indices used to interpret palaeoredox conditions in ancient mudstones: Chemical Geology, v. 111, p. 111–129.

Kidder, D.L., and D.H. Erwin, (2001). Temporal distribution of biogenic silica through the Phanerozoic: comparison of silica-replaced fossils and bedded cherts at the series level: Journal of Geology, v. 109, p. 509–522.

Kochenov, A.V., K.G. Korolev, V.T. Dubinchuk, and Y.L. Medvedev, (1977). Experimental data on the conditions of uranium precipitation from aqueous solutions: Geochemistry International, v. 14, p. 82–87.

Ladipo, K.O., (1988). Palaeogeography, sedimentation and tectonics of the upper cretaceous Anambra Basin, Southeastern Nigeria: Journal of African Earth Sciences, v. 7, p. 865-871.

Lewan, M.D. and J.B. Maynard, (1982). Factors controlling enrichment of vanadium and nickel in the Bitumen of organic sedimentary rocks: Geochimica et Cosmochimica Acta, v. 46, p. 2541–2560. https://doi.org/10.1016/0016-7037(82)90377-5

Liu, Y.J., L.M. Cao, Z.L. Li, H.N. Wang, T.Q. Chu, and J. R. Zhang, (1984). Elemental geochemistry: Science Press, Beijing, China, p. 1–80.

Mamman, Y. D., E. F. C. Dike, I. V. Haruna, and A. I. Haruna, 2010, Clay Mineralogy And Paleodepositional Environments Of Late Cenomanian-turonian Sediments In The Yola Arm, Upper Benue Trough, North Northeastern Nigeria: Journal of Mining and Geology, v.46, n. 2.

Martinez-Ruiz, F., M. Kastner, A. Paytan, M. Ortega-Huertas, and S.M. Bernasconi, (2000). Geochemical evidence for enhanced Productivity during S1 sapropel deposition in the eastern Mediterranean: Paleoceanography v. 15, p. 200–209.

McManus, J., W.M. Berelson, D.E. Hammond, and G.P. Klinkhammer, (1999). Barium cycling in the North Pacific: Implication for the utility of Ba as a paleoproductivity and paleoalkalinity proxy: Paleoceanography, v. 14, p. 62–73.

McManus, J., W.M. Berelson, G.P. Klinkhammer, K.S. Johnson, K.H. Coale, R.F. Anderson, N. Kumar, D.J. Burdige, D.E. Hammond, H.J. Brumsack, D.C. McCorckle, and A. Rushdi, (1998a). Geochemistry of barium in marine sediments: implications for its use as a paleoproxy: Geochimica et Cosmochimica Acta, v. 62, p. 3453–3473.

McManus, J., W.M. Berelson, G.P. Klinkhammer, T.E. Kilgore, and D.E. Hammond, (1998b). Remobilisation of barium in continental margin sediments: Geochimica et Cosmochimica Acta, v. 58, p. 4899–4908.

Meng, Q.T., Z.J. Liu, A.A., Bruch, R. Liu, and F. Hu, (2012). Palaeoclimatic evolution during Eocene and its influence on oil shale mineralisation, Fushun Basin: China. Journal of Asian Earth Sciences, v. 45, p. 95–105. https://doi.org/10.1016/j.jseaes.2011.09.021

Monnin, C., C. Jeandel, T. Cattaldo, and F. Dehairs, (1999). The marine barite saturation state of the world's oceans: Marine Chemistry, v. 65, p. 253–261.

Morford, J.I. and S. Emerson, (1999). The geochemistry of redox-sensitive trace metals in sediments. Geochimica et Cosmochimica Acta, v. 63, p. 1735-1750. https://doi.org/10.1016/S0016-7037(99)00126-X

Morford, J.L., A.D. Russell, and S. Emerson, (2001). Trace metal evidence for changes in the redox environment associated with the transition from terrigenous clay to diatomaceous sediment, Saanich Inlet, BC: Marine Geology, v. 174, p. 355–369.

Murphy, A.E., B.B. Sageman, D.J. Hollander, T.L. Lyons, and C.E. Brett, (2000). Black shale deposition and faunal overturn in the Devonian Appalachian Basin: clastic starvation, seasonal water-column mixing, and efficient biolimiting nutrient recycling: Paleoceanography, v. 15, p. 280–291.

Ojo, O.J., A. U. Kolawole, and S.O. Akande, (2009). Depositional environments, organic richness and petroleum generating potential of the Campanian to Maastrichtian Enugu Formation, Anambra basin: Nigeria: Pacific Journal of Science and Technology, v. 10, no. 1, p. 614-627. (Published by Akamai University, USA, http://www.akamaiuniversity.us/PJST.htm).

OJO, O.J., O.A. Hameed and B. Alalade, 2010, the sedimentary lithofacies, paleoenvironments and hydrocarbon source rock facies of the Eze-Aku Formation, Lower Benue Trough, Nigeria: The Icfai University Journal of Earth Sciences, v. 4, p.7–22. (Published by The Icfai University Press, India, http://www.iupindia.org).

Pearce, T. J., D.S. Wray, K. T. Ratcliffe, D. K. Wright, and A. Moscarello, (2005). Chemostratigraphy of the Upper Carboniferous Schooner Formation, southern North Sea. In: Carboniferous hydrocarbon

geology: the southern North Sea and surrounding onshore areas. In Collinson, J. D., Evans, D. J., Holliday, D. W., & Jones N. S. (Eds.), Yorkshire Geological Society, Occasional Publications series (v. 7, p. 147–64).

Piper, D.Z., and R.B. Perkins, (2004). A modern vs Permian black shale—the hydrography, Primary Productivity, and water-column deposition chemistry: Chemical Geology, v. 206, p. 177–197.

Ramkumar, M., and G. Sathish, (2006). Integrated sequence and chemostratigraphic modeling: A sure-fire technique for stratigraphic correlation, petroleum exploration and reservoir characterization. In Rajendran, S., Srinivasamoorty, K., & Aravindan, S. (Eds.), Mineral Exploration: Recent Strategies, p. 21–40. New India Publishers.

Ratcliffe, K. T., A. M. Wright, P. Montgomery, A. Palfrey, A. Vonk, J. Vermeulen, and M. Barrett, (2010). Application of chemostratigraphy to the Mungaroo Formation, the Gorgon Field, offshore Northwest Australia: APPEA Journal 2010 50th Anniversary Issue, p. 371 – 385.

Ratcliffe, K. T., A. Morton, D. Ritcey, and C. E. Evenchick, (2007). Whole rock geochemistry and heavy mineral analysis as exploration tools in the Bowser and Sustut Basins, British Colombia, Canada: Journal of Canadian Petroleum Geology, v. 55, p. 320–37. http://dx.doi.org/10.2113/gscpgbull.55.4.320.

Rimmer, S.M., J.A. Thompson, S.A. Goodnight, and T.L. Robl, (2004). Multiple controls on preserving organic matter in Devonian–Mississippian marine black shales: geochemical and petrographic evidence: Palaeogeography, Palaeoclimatology and Palaeoecology, v. 215, p. 125–154.

Riquier, L., N. Tribovillard, O. Averbuch, M.M. Joachimski, G. Racki, X. Devleeschouwer, A. El Albani, and A. Riboulleau, (2005). Productivity and bottom water redox conditions at the Frasnian–Famennian boundary on both sides of the Eovariscan Belt: constraints from trace element geochemistry. In: Over, D.J., Morrow, J.R., Wignall, P.B. (Eds.), Understanding Late Devonian and Permian–Triassic Biotic and Climatic Events: Towards an Integrated Approach: Developments in Palaeontology and Stratigraphy, Elsevier Pub. Co., p. 199–224.

Ross, D.J.K., R.M. Bustin, (2006). Sediment geochemistry of the Lower Jurassic Gordondale Member, northeastern British Columbia: Canadian Petroleum Geology, v. 54, p. 337–365.

Ryo Matsumoto, & Azuma Iijima. (1981). Origin and diagenetic evolution of Ca–Mg–Fe carbonates in some coalfields of Japan. Sedimentology, 28(2), 239–259. https://doi.org/10.1111/j.1365-3091.1981.tb01678.x

Schieber, J., (1996). Early diagenetic silica deposition in algal cysts and spores: a source of sand in black shales: Journal of Sedimentary Research, v. 66, p. 175–183.

Schieber, J., D. Krinsley, and L. Riciputi, (2000). Diagenetic origin of quartz silt in mudstones and implications for silica cycling: Nature (London), v. 406, p. 981–985.

Schreiber, B. C. (ed.) (1988). Evaporites and Hydrocarbons: New York: Columbia University Press. 475p. ISBN 0 231 06530 2.

Shearman, D.J., (1983), Syndepositional and late diagenetic alteration of primary gypsum to anhydrite: 6th Int. Symp. Salt, v. 1, no. 41-50.

Shi, J.A., X.L. Guo, Q. Wang, N.Z. Yan, and J.X. Wang, (2003). Geochemistry of REE in QH1 Sediments of Qinghai Lake since Late Holocene and Its Paleoclimatic Significance. Journal of Lake Sciences, v. 15, no. 1, p. 28-33. [in Chinese with English abstract]

Srinivasan, M. S. (1989). Recent advances in Neogene planktonic foraminiferal biostratigraphy, chemostratigraphy and paleoceanography, Northern Indian Ocean: Journal of Palaeontological Society of India, v. 34, p. 1–18.

Taylor, S.R., (1964). The abundance of chemical elements in the continental crust–a new table: Geochimica et Cosmochimica Acta 28, p. 1273–1285.

Teng, G.E., W.H. Liu, Y.C. Xu, and J.F. Chen, (2005). Correlative study on parameters of inorganic geochemistry and hydrocarbon source rocks formative environment: Advances in Earth Sciences, v. 20, no. 2, p. 193-200 (in Chinese with English abstract).

Torres, M.E., H.J. Brumsack, G. Bohrman, and K.C. Emeis, (1996). Barite front in continental margin sediments: a new look at barium remobilisation in the zone of sulfate reduction and formation of heavy barites in diagenetic fronts: Chemical Geology, v. 127, p. 125–139.

Tribovillard, N., A. Riboulleau, T. Lyons, and F. Baudin, (2004). Enhanced trapping of molybdenum by a sulfurised organic matter of marine origin as recorded by various Mesozoic formations: Chemical Geology, v. 213, p. 385–401.

Tribovillard, N., J.-P., Caulet, C. Vergnaud-Grazzini, N. Moureau, and P. Tremblay, (1996). Geochemical study of a glacial transition in the upwelling influenced Somalia margin, N-W Indian Ocean: an unexpected lack of organic matter accumulation: Marine Geology, v. 133, p. 157–182.

Tribovillard, N., T.J. Algeo, T. Lyons, and A. Riboulleau, (2006). Trace metals as paleoredox and paleoproductivity proxies: an update: Chemical Geology, v. 232, p. 12–32.

Van Os, B.J.H., Middelburg, J.J., and G.J. de Lange, (1991). Possible diagenetic mobilisation of barium in sapropelic sediments from the eastern Mediterranean: Marine Geology, v. 100, p. 125–136.

Van Santvoort, P.J.M., G.J. de Lange, J. Thomson, H. Cussen, T.R.S. Wilson, M.D. Krom, and K. Ströhle, (1996). Active postdepositional oxidation of the most recent sapropel (S1) in the eastern Mediterranean Sea sediments: Geochimica et Cosmochimica Acta, v. 60, p. 4007–4024.

Wang, Y.Y., W.Y. Guo, and G.D. Zhang, (1979). Application of some geochemical indicators in determining the sedimentary environment of the Funing Group (Paleogene), Jin-Hu Depression, Kiangsu Province: Journal of Tongji University, v. 2, p. 51–60. [in Chinese with English abstract]

Wang, Z.M., (2003). Geochemical indicators for diagnosing anoxic sedimentary environment: Acta Geologica Gansu, v. 12, no. 2, p. 55–58. [in Chinese with English abstract]

Wignall, P.B., and Myers, K.J., (1988). Interpreting benthic oxygen levels in mudrocks: a new approach: Geology, v. 16, p. 452–455.

Wignall, P.B., and Twitchett, R.J., (1996). Oceanic anoxia and the end Permian mass extinction, Science, v. 272, p. 1155–1158.

Wright, A.M., K. Ratcliffe, S. Zaitlin, S.W. David, (2010). The Application of Chemostratigraphic Techniques to Distinguish Compound Incised Valleys in Low-Accommodation Incised-Valley Systems in a Foreland-Basin Setting An Example from the Lower Cretaceous Mannville Group and Basal Colorado Sandstone (Colorado Group), Western Canadian Sedimentary Basin. DOI: 10.2110/sepmsp.094.093